



## Differential pattern of neurotoxicity induced by the gliadin peptides p31-43 and p57-68 in *in vitro* model of epilepsy

Elisabetta Gerace<sup>a,b,\*</sup>, Francesco Resta<sup>a,1</sup>, Lorenzo Curti<sup>a</sup>, Alessandro Di Domizio<sup>c</sup>, Giuseppe Ranieri<sup>a</sup>, Matteo Becatti<sup>d</sup>, Daniela Renzi<sup>d</sup>, Antonino Calabrò<sup>d</sup>, Guido Mannaioni<sup>a</sup>

<sup>a</sup> Department of Neurosciences, Psychology, Drug Research and Child Health, University of Florence, Italy

<sup>b</sup> Department of Health Sciences (DSS), University of Florence, Florence, Italy

<sup>c</sup> SPILLOproject, Milano, Italy

<sup>d</sup> Department of Experimental and Clinical Biomedical Sciences "Mario Serio", University of Florence, Firenze, Italy

### ARTICLE INFO

#### Keywords:

Gliadin peptides  
Kainate  
Organotypic hippocampal slices  
Neurotoxicity  
MAPK  
NfκB

### ABSTRACT

Epilepsy is a central nervous system (CNS) disorder causing repeated seizures due to a transient excessive or synchronous alteration in the electrical activity of the brain. Several neurological disorders have been associated to gluten-related diseases (GRD), including epilepsy. However, the molecular mechanisms that associate GRD and epileptogenesis are still unknown. Our previous data have shown that the gliadin peptide 31–43 (p31-43) enhanced number and duration of seizures induced by kainate in mice and exacerbated CA3-kainate-induced neurotoxicity in organotypic hippocampal slices. Here, we investigated whether another important gliadin peptide p57-68 may exert effects similar to p31-43 on kainate-induced neurotoxicity. We find that both peptides exacerbate kainate-induced damage in the CA3 region once simultaneously challenged. However, after pre-incubation, p31-43 additionally exacerbates neurotoxicity in the CA1 region, while p57-68 does not. These data suggested differential intracellular mechanisms activated by the peptides. Indeed, analysing intracellular signalling pathways we discover that p31-43 induces significant intracellular changes, including increased phosphorylation of Akt, Erk1/2, and p65, decreased p38 phosphorylation, and deacetylation of nuclear histone-3. Based on these observations, we demonstrate that p31-43 likely activates specific intracellular signaling pathways involved in neuronal excitability, inflammation, and epigenetic regulation, which may contribute to its exacerbation of kainate-induced neurotoxicity. In contrast, p57-68 appears to exert its effects through different mechanisms. Further research is necessary to elucidate the precise mechanisms by which these peptides influence neurotoxicity and understand their implications for neurological disorders.

### 1. Introduction

Epilepsy is a neurological disorder characterized by recurring and unprovoked seizures, affecting millions of individuals worldwide. The condition arises from abnormal brain activity, often resulting from imbalances in neurotransmitters or disruptions in ion channels. Seizures can manifest in various forms, including convulsions, loss of consciousness, or altered sensations. The underlying causes of epilepsy are

diverse and can stem from genetic factors, brain injuries, infections, or developmental abnormalities [1]. Understanding the mechanisms and contributing factors of epilepsy is crucial for improved diagnosis, treatment, and management of this debilitating condition. The connection between celiac disease (CD) and gluten sensitivity (GS) with neurological manifestations have been largely described [2–4] and gluten-related neurological disorders (GRND) may enter as a new clinical terminology describing patients that present GS and neurological

**Abbreviations:** CNS, Central Nervous System; GRD, Gluten-Related Diseases; p31-43, gliadin peptide 31-43; p57-68, gliadin peptide p57-68; CD, Celiac Disease; GS, Gluten Sensitivity; GRND, Gluten-Related Neurological Disorders; TLE, Temporal Lobe Epilepsy; IL-15, interleukin-15; PI, Propidium iodide; TG2, Transglutaminase 2.

\* Corresponding author at: Department of Health Sciences (DSS), University of Florence, Viale G. Pieraccini 6, 50139 Florence, Italy.

E-mail address: [elisabetta.gerace@unifi.it](mailto:elisabetta.gerace@unifi.it) (E. Gerace).

<sup>1</sup> Present address: European Laboratory for Non-linear Spectroscopy, University of Florence, 50019 Sesto Fiorentino, Italy; Department of Physics and Astronomy, University of Florence, 50019 Sesto Fiorentino, Italy.

<https://doi.org/10.1016/j.bcp.2024.116409>

Received 8 November 2023; Received in revised form 11 June 2024; Accepted 2 July 2024

Available online 3 July 2024

0006-2952/© 2024 The Authors. Published by Elsevier Inc. This is an open access article under the CC BY-NC-ND license (<http://creativecommons.org/licenses/by-nc-nd/4.0/>).

presentations. In particular, the prevalence of epilepsy in patients with CD is 1.8 times more common and CD is over 2 times more prevalent in patients with epilepsy, compared to the general population [5]. In the context of GRND, epileptic seizures presenting encompass the full spectrum of epilepsy, with higher amongst particular epileptic presentations including temporal lobe epilepsy (TLE) with hippocampal sclerosis and cerebral calcification [6,7]. Importantly, gluten restriction diet is effective in the management of epilepsy, either reducing seizure frequency and decreasing antiepileptic medications, needed to control intractable seizures in humans [8,9]. Several hypotheses have been proposed to elucidate the relationship between epilepsy and gluten-related neurological disorders (GRND), including gluten toxicity [10], autoimmune mechanisms [11], and malabsorption [7]. However, despite extensive research, there is currently no evidence establishing a causal link between epilepsy and GRND. The question of whether gluten plays a contributory role in the pathogenesis of these disorders or merely represents an epiphenomenon remains unanswered. Further investigations are warranted to unravel the complex mechanisms underlying the association between epilepsy and GRND and determine the precise involvement of gluten in their development.

Kainic acid is a potent neurotoxin extensively utilized in experimental settings to generate seizures through activation of its own glutamate kainate receptors (KARs). In fact, extensive evidence demonstrated that both systemic and intracerebral administration of kainate in animals lead to activity-induced neuronal and cell loss, astrogliosis, and hippocampal sclerosis of CA1 and CA3 pyramidal cells, which elicits behavioral and electrophysiological seizures, similar to those observed in human with TLE [12,13,14,15,16]. Moreover, CA3 pyramidal neurons are indeed amongst the most responsive neurons to kainate in the brain and also the hippocampal pacemaker for the generation of synchronized activities that subsequently propagate to CA1 and other brain regions [14].

Amongst the gliadin fragments that remain undigested by the intestine [17] and that have been implicated in triggering immune responses in CD patients, the gliadin peptides 31-43 (p31-43) and 57-68 (p57-68) (Fig. 1) have attracted attention for their differential effects on immune response or toxic reaction, leading to the clinical consequences related to CD and GS [17,18]. In particular, p31-43 is the prototype of peptides

effective on innate response that has been shown to be toxic both in *in vitro* and *in vivo* tissues obtained from patients with CD [19,20]. Additionally, p31-43 is able to initiate both stress and innate immune responses with interleukin-15 (IL-15) as a major mediator in celiac intestine. P31-43 also upregulates ICAM1 and HLA molecules and it is responsible for the activation of dendritic cells, determined by the expression of CD83 [21]. Furthermore, its particular conformation and its ability to induce different forms of cellular stress may determine the activation of numerous signalling pathways, which, in the presence of appropriate susceptibility and environmental factors, may act together to drive diseases [22]. Differently, p57-68 is a small fragment of gliadin that is critical in the induction of the adaptive immune response and it is one of the dominant epitopes recognized by T cells isolated from the intestine of CD patients. Studies have shown that p57-68 can bind to a specific receptor on the surface of immune cells called human leukocyte antigen (HLA)-DQ2 or HLA-DQ8, which then triggers an adaptive immune response [23]. This interaction is thought to be a key step in the development of CD.

Unfortunately, studies on understanding the potential relationship between the gliadin peptides and epilepsy are lacking. A recent paper from our laboratory have demonstrated the neurotoxic effect of p31-43 on kainate-induced seizures in an *in vivo* model of epilepsy. In particular, our results showed that the gliadin peptide p31-43 does not provoke convulsions *per se*, while the administration of p31-43 in C57/Bl6 mice exacerbated the number and the duration of seizures induced by kainate, reproducing what has been widely observed in many clinical case in humans [9]. In addition, p31-43 exacerbated kainate neurotoxicity, through the involvement of the enzymatic activity of transglutaminases [24].

The primary objective of this study is to examine the impact of p31-43 and p57-68 on kainate-induced neurotoxicity and the corresponding intracellular mechanisms triggered by these gliadin-derived peptides. By elucidating their cellular effects, this research aims to shed light on the potential mechanisms that contribute to the heightened sensitivity to harmful stimuli observed in individuals with epilepsy and gluten sensitivity. This research will provide insights into the potential interactions between epilepsy and gluten sensitivity, helping to advance our understanding of their interconnected pathophysiological processes.

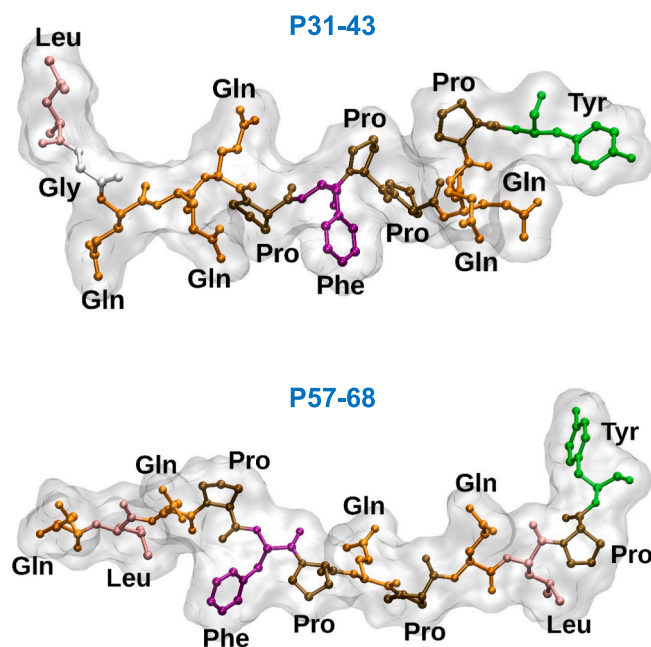


**Fig. 1.** 3D representation of the gliadin peptides p31-43 (LGQQPPFPQPY) and p57-68 (QLQPPFPQLPY). The p31-43 reported conformation corresponds to the first model of the NMR multi-model PDB file '6QAX, while the conformation of p57-68 was generated randomly' (drawings rendered using VMD [44]).

## 2. Materials and methods

Male and female Wistar rats were obtained from Charles River (MI, Italy). Animals were housed at  $23 \pm 1$  °C under a 12 h light–dark cycle (lights on at 07:00) and were fed a standard laboratory diet with ad libitum access to water. The experimental protocol was approved by the Italian Ministry of Health (Aut. 176; 17E9C.N.VAS) and the European Communities Council Directive of 2010/63/EU. The authors further attest that all efforts were made to minimize the number of animals used and their suffering.

### 2.1. Materials

Kainic acid and Propidium iodide (PI) were purchased from Sigma (St Louis, MO, USA), synthetic peptide p31–43 (LGQQQPFPPQPPY) and synthetic peptide p57–68 (QLQPFPPQLPY) were purchased from Primm S.r.l., (Milan, Italy), Tissue culture reagents were obtained from Gibco-BRL (San Giuliano Milanese, MI, Italy) and Sigma (St Louis, MO, USA).

## 3. Methods

### 3.1. Organotypic hippocampal slice preparation

Organotypic hippocampal slice cultures were prepared as previously reported [25]. Briefly, hippocampi were removed from the brains of 7- to 9-day old male and female Wistar rat pups (totalling approximately 167 animals) (Harlan, MI, Italy). Transverse slices (420  $\mu$ m) were prepared using a McIlwain tissue chopper and then transferred onto 30 mm diameter semiporous membranes inserts (Millicell-CM PICM03050; Millipore, Italy), which were placed in six well tissue culture plates containing 1.2 ml medium per well. The culture medium consisted of 50 % Eagle's minimal essential medium, 25 % heat-inactivated horse serum, 25 % Hanks' balanced salt solution, 5 mg/ml glucose, 2 mM L-glutamine, and 3.75 mg/ml amphotericin B. Slices were maintained at 37 °C in an incubator in atmosphere of humidified air and 5 % CO<sub>2</sub> for two weeks. Before experiments, all slices were screened for viability by phase-contrast microscopy analysis; slices displaying signs of neurodegeneration were discarded from the study.

### 3.2. p31-43 and p57-68 exposure in organotypic hippocampal slice model of epilepsy

The experiments were conducted as previously described in Gerace et al. (2017) [24]. Briefly, after 2 weeks in culture, the slices were exposed to 5  $\mu$ M kainate for 24 h, which is considered a classical model of temporal epilepsy [26]. Under these conditions, the slices undergo selective injury of the CA3 pyramidal cells. We have tested the effects of the gliadin p31-43 (30  $\mu$ g/ml) and p57-68 (10–100  $\mu$ g/ml) by adding the peptides to the incubation medium for 60 min alone (pre-incubation) and then during the 24 h exposure to kainate or only during the 24 h exposure to kainate (co-incubation).

### 3.3. Assessment of hippocampal cell injury

At the end of the experiments, the slices were assessed for neuronal injury by measuring the intensity of propidium Iodide (PI) fluorescence. PI (5  $\mu$ g/ml) was added to the medium and thirty minutes later, fluorescence was viewed using an inverted fluorescence microscope (Olympus IX-50; Solent Scientific, Segensworth, UK) equipped with a xenon-arc lamp, a low-power objective (4X) and a rhodamine filter. Images were digitized using a video image obtained by a CCD camera (Diagnostic Instruments Inc., Sterling Heights, MI, USA) controlled by software (InCyt Im1TM; Intracellular Imaging Inc., Cincinnati, OH, USA) and subsequently converted using the Image-Pro Plus morphometric analysis software (Media Cybernetics, Silver Spring, MD, USA). In

order to quantify cell death, the CA3 and CA1 hippocampal subfield was identified and encompassed in a frame using the drawing function in the image software (ImageJ; NIH, Bethesda, USA) and the optical density of PI fluorescence was detected. There was a linear correlation between CA3/CA1 PI fluorescence and the number of injured CA3/CA1 pyramidal cells as detected by morphological criteria [27,28].

### 3.4. Preparation of protein extracts and western blot analyses

The experiments were performed as previously reported in [29] and [28]. Hippocampal slices were exposed to 30  $\mu$ g/ml p31-43 or 30  $\mu$ g/ml p57-68 for 30, 60 or 180 min before western blotting analysis. At the end of the experiments, cultured slices were washed with cold 0.01 M phosphate-buffered saline, pH 7.4 and 8 slices/sample were gently transferred and dissolved in a tube containing 1 % SDS. Total protein levels were quantified using the Pierce (Rockford, IL, USA) BCA (bicinchoninic acid) Protein Assay. Forty  $\mu$ g of proteins were resolved by electrophoresis on a 4–20 % SDS-polyacrylamide gel and transferred onto nitrocellulose membranes using the transblot TURBO (Bio-Rad, Hercules, CA, USA). Blots were probed overnight at 4 °C with the polyclonal rabbit phopsho-Akt (Ser 473), phopsho-Erk1/2 (Thr202/Thr204), phopsho p38, phopsho-p65 (NFkB) and Acetyl-H3 (K18) antibodies; all diluted 1:1000. Immunodetection was performed with secondary antibodies (1:2000 anti-rabbit IgG from donkey (Amersham Biosciences, UK) conjugated to horseradish peroxidase. Tubulin was used as loading control. The reactive bands were detected using chemiluminescence (ECLplus; Euroclone, Padova, Italy). Quantitative analysis was performed using the QuantityOne analysis software (Bio-Rad, Hercules, CA, USA).

### 3.5. Determination of lipoperoxidation levels

Lipoperoxidation products were measured using an ALDetect Lipid Peroxidation Assay (Enzo Life Sciences Inc.) in accordance with the manufacturer's instructions. Briefly, the adduct generated by reacting N-Methyl-2-phenylindole with Malondialdehyde after 2 h at 45 °C was measured spectrometrically in a 96-well microtiter plate reader (Biotek Synergy H1) at 586 nm. Lipoperoxidation products were expressed in terms of malondialdehyde equivalent normalized for protein concentration (nmol/mg).

### 3.6. Total antioxidant capacity (TAC) assay

TAC was assessed using the Oxygen Radical Absorbance Capacity (ORAC) assay following the ORAC manufacturer Zen-Bio's protocol (Zen-Bio, Inc. Durham, USA). Fluorescence was measured with excitation at 485 nm and emission at 538 nm in a 96-well microtiter plate reader (Biotek Synergy H1). Results were expressed as Trolox Equivalents ( $\mu$ M Trolox)/mg of proteins.

### 3.7. Fourier Transform Infrared (FTIR) spectroscopy

For FTIR measurements in attenuated total reflection (ATR), 10  $\mu$ L of p31-43 (0.03 mg/ml) were deposited on the diamond plate of the single reflection ATR device and the spectra were recorded after solvent evaporation as previously described [30] with the FTIR spectrometer (IRXross™, SHIMADZU Corporation, Japan) in the 4000–450 cm<sup>-1</sup> region. The measurements were acquired in a transmission mode with 4 cm<sup>-1</sup> resolution. The spectral data were collected using IRsolution software and then exported as ASCII format for image processing.

### 3.8. Circular dichroism (CD) spectroscopy

CD spectra of p31-43 (0.03 mg/ml) were recorded on a Jasco Fluorimeter (Jasco 810) at 25 °C in 0.2 cm quartz cell from 350 to 180 nm (far UV). Three spectra recorded for each sample. The molar ellipticity

[q] values were calculated according to the equation:  $[\theta]$  (deg-cm<sup>2</sup> dmol<sup>-1</sup>) =  $[\theta$  (MRW)]/[10(l)(c)], where  $\theta$  is the shift from the base value X to the entire range in degrees; MRW is the average weight of amino acid residues; (l) is the cell path length (cm); and (c) is the protein concentration (g/ml).

### 3.9. Intrinsic fluorescence (IF) spectroscopy

In order to evaluate any conformational changes in protein tertiary structure, we provided Intrinsic Fluorescent Spectra. Fibrinogen IF is caused by the presence of three amino acids residues that are intrinsically fluorescent in the aromatic side chain. p41-43 (0.03 mg/ml) spectra has detected spectrophotometrically in a 1 cm quartz cells on an Agilent Cary Eclipse Fluorescence Spectrophotometer at 25 °C by exciting the protein with 280 nm ultraviolet light and an emission wavelength from 290 to 500 nm. Three spectra were acquired for each sample.

### 3.10. Statistical analysis

Data are presented as means  $\pm$  SEM of n experiments from independent cell preparations. Each experimental point consisted of 40 hippocampal slices. Statistical significance of differences between PI fluorescence was evaluated by performing one-way ANOVA followed by Tukey's w test for multiple comparisons for unpaired samples. Statistical significance of differences between Western blot optical densities was assessed with a Student's t-test (unpaired samples) or evaluated by performing one-way ANOVA followed by Dunnett's w test for multiple comparisons for unpaired samples, respectively. Differences were

considered significant for \*p < 0.05, \*\*p < 0.01 and \*\*\*p < 0.001. All statistical calculations were performed using GRAPH-PAD PRISM v.8 for Windows (GraphPad Software).

## 4. Results

### 4.1. p57-68 exacerbates kainate-induced CA3 neurotoxicity

In a previous paper from our laboratory, we examined the effects of the gliadin peptide 31–43 in *in vivo* and *in vitro* models of kainate-induced-epilepsy and we demonstrated that p31-43 increases kainate-induced seizure *in vivo* and exacerbates the kainate-induced CA3 neurotoxicity *in vitro* [24]. Here, we tested whether p57-68 may have similar effects to p31-43 *in vitro*. Therefore, organotypic hippocampal slices were exposed to p57-68 (10–100  $\mu$ g/ml) together with kainate (5  $\mu$ M, 24 h) (co-incubation) or to p31-43 (30  $\mu$ g/ml), used as positive control. Accordingly, with our previous published results [19], the co-incubation of p31-43 plus kainate exacerbated the kainate-induced CA3 damage (Fig. 2, panel B and grey column panel C). We obtained similar results by incubating the slices with p57-68 at same concentration (Fig. 2, panel B and white column panel C), indicating that both peptides provoke increased CA3-kainate-induced neurotoxicity.

### 4.2. Differential effects of p31-43 and p57-68 pre-incubation on kainate neurotoxicity

Assuming that gluten peptides may be present before seizure events in humans, we studied the effects of pre-incubation with either p31-43 or p57-68 on kainate-induced neurotoxicity paradigm *in vitro*,

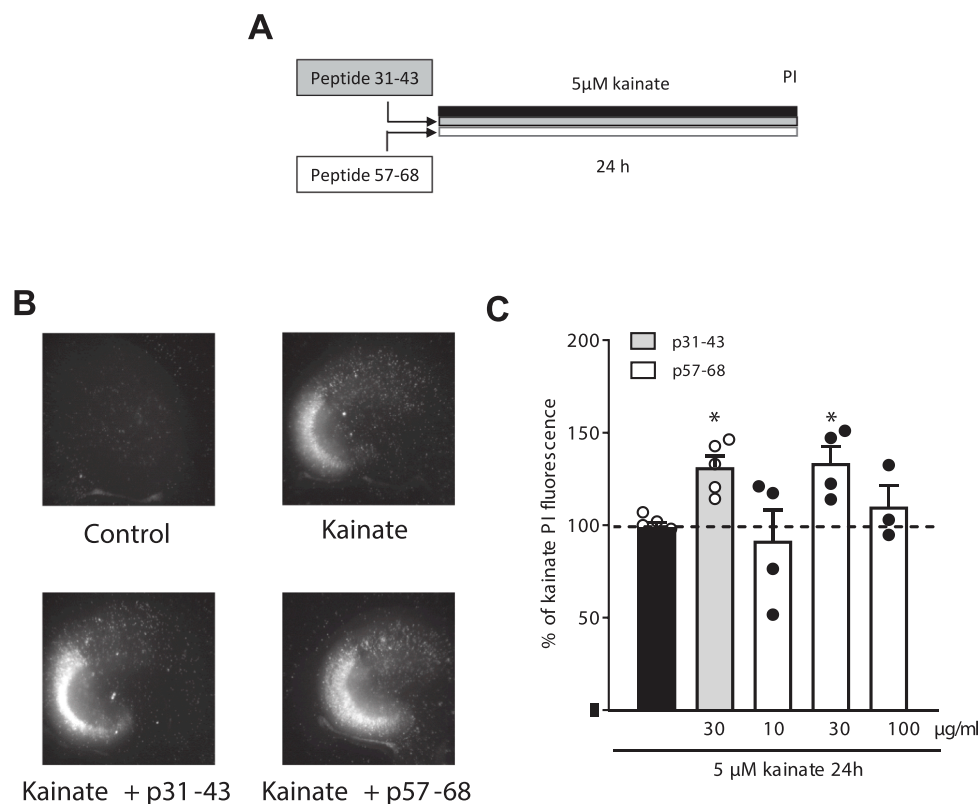


**Fig. 2.** Exacerbation of kainate-induced neurotoxicity by the gliadin peptides p31-43 and p57-68 in an *in vitro* model of epilepsy. (A-B) Experimental protocol showing rat organotypic hippocampal slices incubated for 24 h with 5  $\mu$ M kainate, or with p31-43 (30  $\mu$ g/ml; grey column) or p57-68 (10–100  $\mu$ g/ml; white columns) + kainate and then, incubated with propidium iodide (PI) and observed under fluorescence optics to detect neuronal injury. Kainate toxicity in the CA3 region was exacerbated by 30  $\mu$ g/ml p31-43 and p57-68. (C) Quantitative analysis is expressed as percentage of damage produced by 5  $\mu$ M kainate. Bars represent the mean  $\pm$  SEM of at least four experiments from independent cell preparations (about  $\geq$  24 slices for each experimental point). \*p < 0.5 vs. kainate (ANOVA + Tukey's w test).

hypothesizing that the peptide may provoke different responses from neuronal cells. Hence, organotypic hippocampal slices were exposed to p31-43 or p57-68 (30 µg/ml) alone for 60 min (pre-incubation) and then maintained in the medium together with kainate (5 µM, 24 h) or incubated only during the 24 h exposure to kainate (co-incubation). Again, the co-incubation with p31-43 (Fig. 3A, panel B and grey column panel C) and with p57-68 (Fig. 3B, panel B and white column black circles panel C) exacerbated the kainate-induced CA3 damage (Fig. 3A and 3B, respectively). Interestingly, pre-incubation of p31-43 (but not p57-68) exacerbated kainate-neurotoxicity not only in CA3 region, but also in CA1 region thus suggesting an increase neuronal vulnerability induced by p31-43 but not by 57–68 inducing an enhanced neurodegeneration.

#### 4.3. p31-43, but not p57-68, activates MAPK signaling

To deepen the mechanisms behind the different effects of p57-68 and p31-43 we studied major nuclear and cytosolic pathways. In fact, the different amino acid composition of the two peptides (Fig. 1) may cause an interference with different signaling pathways, which, in the presence of appropriate susceptibility, may act together to drive diseases. Hence, we analyzed the MAPK signaling and, in particular, we used phospho-specific antibodies to measure the relative levels of the phosphorylated, active forms of Akt, Erk1/2 and p38 after 30, 60 or 180 min of p31-43 or p57-68 application. Fig. 4 shows that p31-43 induces a significant increase in Akt (panel A) and Erk1/2 (panel B) phosphorylation, with different kinetics of activation. Conversely, p38 results significantly dephosphorylated after p31-43 incubation for 60 min (Fig. 4, panel C). Surprisingly, no effects were observed after application of p57-68 in hippocampal slices in the same experimental conditions. These results indicate that the gliadin fragments p31-43 and p57-68 activate differential cellular signaling and in particular, p31-43 is able to activate principal pathway that regulates several and central processes at cytosolic level.

#### 4.4. Differential effect of p31-43 and p57-68, on NFκB phosphorylation

To explore whether p31-43 and p57-68 may induce alterations at inflammatory levels, we explored the effects of p31-43 and p57-68 after 30, 60 and 180 min incubation on p65 (NFκB) phosphorylation, that is notably an inflammatory protein target. Interestingly, Fig. 5 shows that p31-43, but not p57-68, increases p-65 phosphorylation. These results indicate that p31-43 may activate pro-inflammatory process that may contribute to exacerbation of epilepsy.

#### 4.5. Differential effect of p31-43 and p57-68, on histone acetylation

To explore whether p31-43 and p57-68 may induce alterations at epigenetic levels, we explored the effects of p31-43 and p57-68 after 30, 60 and 180 min incubation on histone 3 (H3) acetylation on lysine (K18); that is considered an epigenetic protein target. Our results show that H3 results significantly deacetylated after p31-43, but not 57–68, application (Fig. 6). These data are indicative of changed epigenetic signaling that may be the basis of explanation for many pathophysiological process.

#### 4.6. P31-43 induces oxidative stress in organotypic hippocampal slices

To evaluate the influence of p31-43 on oxidative status, we assessed lipid peroxidation and total antioxidant capacity in cell lysates. As depicted in Fig. 7 (left panel), there is a notable elevation in lipid peroxidation following only 6 h of p31-43 peptide incubation, escalating to a 3.25-fold increase after 24 h. Concurrently, the temporal profile of total antioxidant capacity (Fig. 7, right panel) indicates the presence of oxidative stress. Notably, a significant decline in total antioxidant capacity is observed after just 1 h of p31-43 incubation, persisting until 3 h, signifying a depletion in antioxidant defenses. Subsequently, the

cellular response attempts to counteract oxidative stress, evident in a sharp increase in antioxidant defenses after 6 h of p31-43 incubation. However, beyond 24 h, the cell's ability to counterbalance the heightened free radical production diminishes significantly, leading to a marked reduction in total antioxidant capacity.

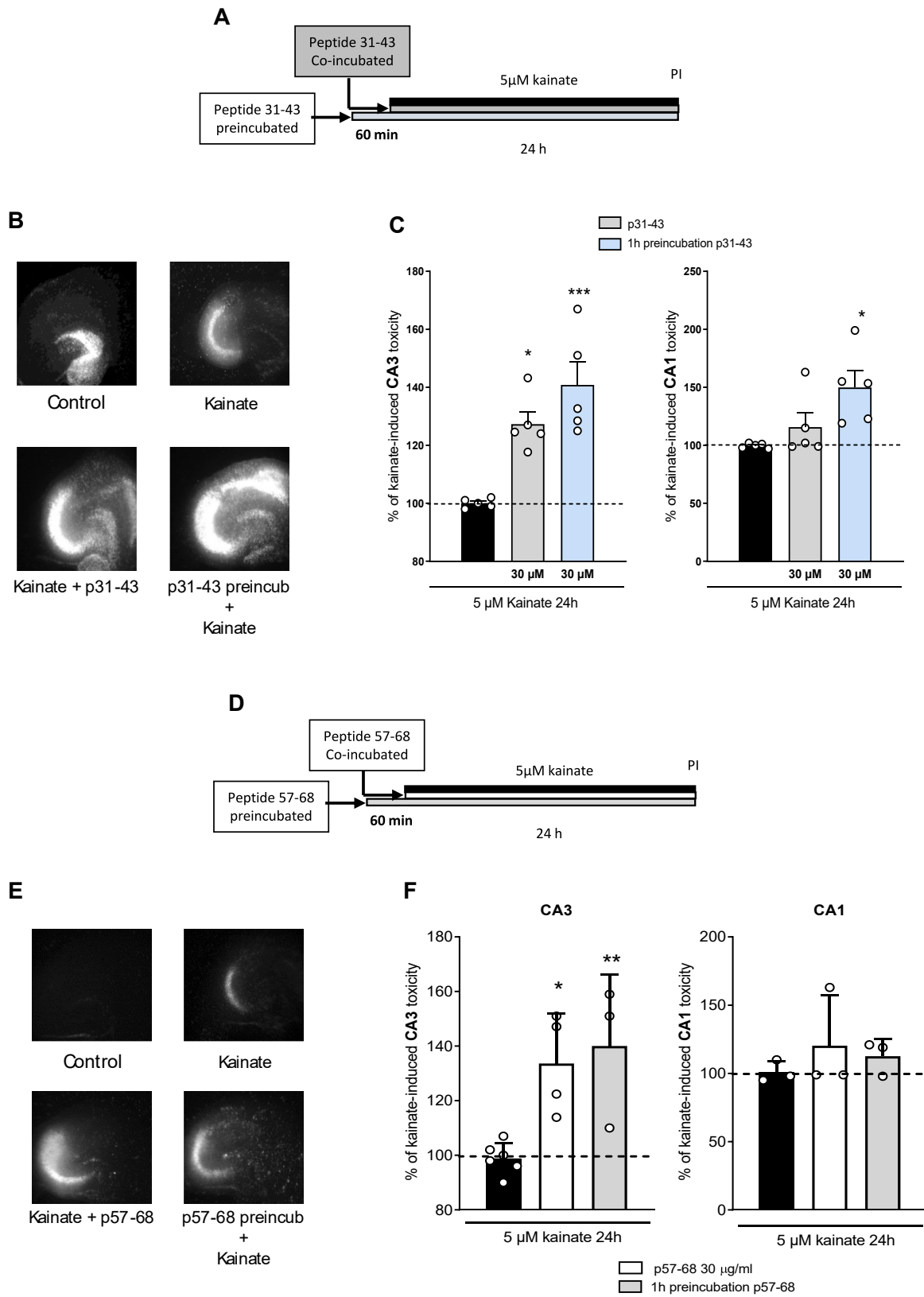
#### 4.7. Structural analysis of p31-43 aggregation

To confirm that the toxic effects induced by the peptide were not due to its potential aggregation, we performed structural analysis using FTIR spectroscopy, circular dichroism (CD), and intrinsic fluorescence (IF) spectroscopy. Our findings (Fig. 8, panel A) clearly show that under our experimental conditions, aggregate formation does not occur. The observed toxic effects after incubation with p31-43 are thus solely due to peptide toxicity rather than the presence of aggregates. Additionally, we examined the secondary structure of p31-43 using CD and IF spectroscopy at T0 and after 24 h of incubation at 37 °C in PBS. As illustrated in Fig. 8 (panel B), the recorded spectra are identical, indicating that the peptide structure remains unchanged and suggesting the absence of an aggregation process.

### 5. Discussion

Emerging evidence suggests a potential link between gluten sensitivity and epilepsy, highlighting the role of dietary factors in neurological disorders [31]. Gluten sensitivity, characterized by adverse reactions to gluten-containing grains, can manifest as celiac disease or non-celiac gluten sensitivity. While celiac disease is well-established as a gluten-related autoimmune condition, its association with epilepsy has also gained attention. Furthermore, non-celiac gluten sensitivity has been implicated in neurological manifestations, including seizures and epilepsy-like symptoms [3]. Understanding the influence of gluten sensitivity on epilepsy is crucial for comprehending the underlying mechanisms, informing diagnostic approaches, and exploring potential dietary interventions to improve epilepsy management.

A recent paper from our laboratory has demonstrated that administration of the gliadin peptide p31-43 in C57/Bl6 mice exacerbates the number and the duration of seizures induced by kainate [24], reproducing what has been widely observed in many clinical cases in humans. Moreover, in the same paper it has been shown that incubation of p31-43 in combination with kainate exacerbated the CA3 hippocampal damage provoked by kainate alone in organotypic hippocampal slices [24]. All these results indicated a relationship between gluten fragments and epilepsy and suggested molecular mechanisms involving the enzymatic activity of transglutaminases and kainate receptor modulations [24]. In this study, we aimed to investigate whether other undigested gliadin fragments in the intestine may exhibit similar effects to those previously observed. Specifically, we focused on examining the peptide p57-68, which shares the same length as p31-43 but possesses a distinct amino acid composition. By exploring the potential effects of p57-68, we sought to broaden our understanding of the biological activity of gliadin fragments and their impact on physiological processes. The gliadin peptides p31-43 and p57-68 have attracted attention for their differential effects on immune response or toxic reaction, leading to the clinical consequences related to CD and GS [17,18]. In particular, p31-43 is the prototype of peptides effective on innate response that has been shown to be toxic both in *in vitro* and *in vivo* tissues obtained from patients with CD [19,20]. Differently, p57-68 is critical in the induction of the adaptive immune response and it is one of the dominant epitopes recognized by T cells isolated from the intestine of CD patients. P57-68 can bind to a specific receptor on the surface of immune cells (called HLA-DQ2 or HLA-DQ8) which then triggers an immune response and this interaction is thought to be a key step in the development of CD [23]. Here, we observed that p-57-68 exerts similar effects to p31-43 on kainate-induced neurotoxicity. Indeed, organotypic hippocampal slices exposed to p57-68 showed increased kainate-induced CA3 damage, as



(caption on next page)

**Fig. 3.** P31-43 but not with p57-68 pre-incubation exacerbates kainate neurotoxicity in CA1 hippocampal region. (3A) A-B. Experimental protocol showing rat organotypic hippocampal slices incubated for 60 min with p31-43 alone (pre-incubation) and then in combination with 5  $\mu$ M kainate for 24 h, or with p31-43 + kainate (co-incubation) and then, incubated with propidium iodide (PI) and observed under fluorescence optics to detect neuronal injury. Kainate toxicity was exacerbated by 30  $\mu$ g/ml p31-43 not only in CA3 but also in CA1 region. (C) Quantitative analysis is expressed as percentage of damage produced by 5  $\mu$ M kainate. Bars represent the mean  $\pm$  SEM of at least four experiments from independent cell preparations (about  $\geq$  24 slices for each experimental point)  $**p < 0.01$  vs. kainate (ANOVA + Tukey's w test). (3B) A-B. Experimental protocol showing rat organotypic hippocampal slices incubated for 60 min with p57-68 alone (pre-incubation) and then in combination with 5  $\mu$ M kainate for 24 h, or with p57-68 + kainate (co-incubation) and then, incubated with propidium iodide (PI) and observed under fluorescence optics to detect neuronal injury. Kainate toxicity was exacerbated by 30  $\mu$ g/ml p57-68 only in CA3 but not in CA1 region. (C) Quantitative analysis is expressed as percentage of damage produced by 5  $\mu$ M kainate. Bars represent the mean  $\pm$  SEM of at least three experiments from independent cell preparations (about  $\geq$  24 slices for each experimental point).  $**p < 0.01$  vs. kainate (ANOVA + Tukey's w test).

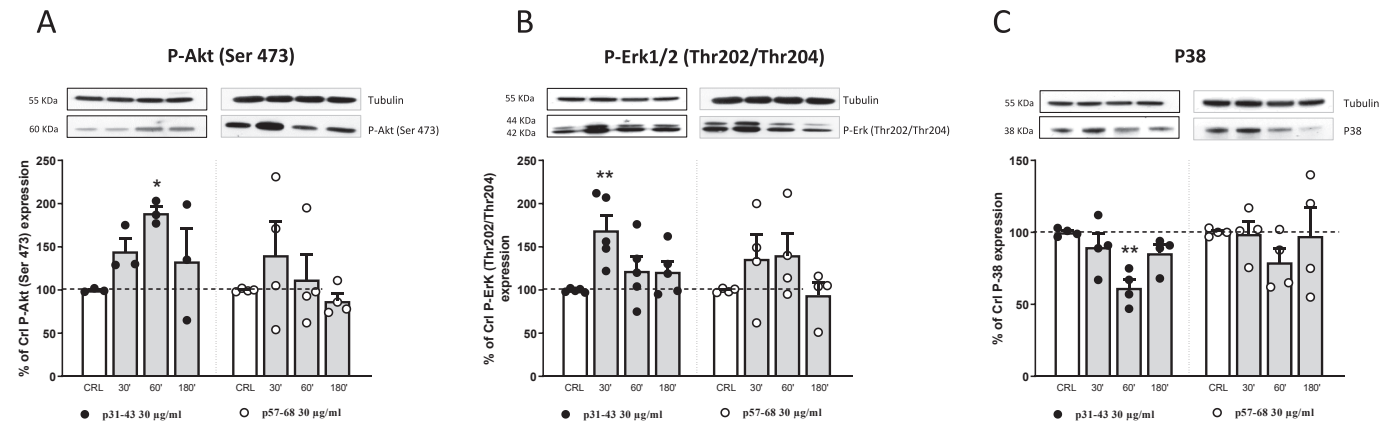


**Fig. 4.** MAPK signalling activation induced by p31-43 but not p57-68. Slices were exposed to p31-43 (grey column black circles) or to p57-68 (grey column white circles) for 30, 60 or 180 min and then processed for Western blotting. Representative immunoblots showing that p31-43 but not p57-68 alters the phosphorylation levels of phospho-Akt (Ser473) (panel A) phospho-ERK1 / 2 (Thr202 / Thr204) (panel B) and phospho-p38 (panel C). Data are expressed as percentage of control protein levels (white column). Bar represent the mean  $\pm$  SEM of three-five experiments from independent cell preparations (about  $\geq$  8 slices for each experimental point).  $**p < 0.01$  and  $*p < 0.05$  versus. CRL (ANOVA + Tukey's w test).

well as p31-43. Conversely, when pre-incubated for 60 min and then together with kainate, the gliadin peptides displayed differential pattern of neurotoxicity. Specifically, p31-43, but not p57-68, enhanced CA3 and CA1 injury. Although the CA4 region is crucial in epilepsy, contributing to seizure onset and spread, and interest in the involvement of the CA2 region in epilepsy has surged recently [32,33], research on their roles in kainate-induced seizures is relatively scarce compared to the extensive studies on CA1 and CA3 hippocampal subfields. Hence, our analysis was centered on the well-established roles of the CA1 and CA3 hippocampal regions in kainate-induced epilepsy.

The neurotoxic effect of p31-43 is solely attributable to peptide toxicity rather than their aggregates, indeed under our experimental conditions, p31-43 aggregate formation does not occur, conversely to what reported by Chirido et al., showing that p31-43 spontaneously forms oligomeric nanostructures driving multiple inflammatory pathways [22]. However, our data are in line with what reported by Calvanese et al., who noticed that p31-43 aggregates are not visible in solution by NMR [34].

Interestingly, we previously shown that the incubation with maize zein, a prolamin protein derived from corn used as control peptide, was not toxic by itself and did not alter kainate-induced CA3 toxicity in the same experimental model and conditions, thus suggesting that specifically p31-43 and p57-68, are responsible for increased kainate induced-damage. We hypothesize that these differential responses against kainate neurotoxicity may be dependent on the presence of specific aminoacids (particularly glutamine) as well as aminoacidic sequences (glutamine and proline), that may determine different peptide conformations causing resistance to enzymatic digestion and/or activation of different signalling pathways. In order to explain whether the observed differential neurotoxic effects may be dependent on differential mechanisms, we examined the effects of p31-43 and p57-68 alone on central cellular signaling both at cytosolic and nuclear levels. In particular, we analysed the expression levels of MAPK proteins (Akt, Erk1/2 and p38),

inflammatory marker (NF $\kappa$ B) and nuclear histone-3 in hippocampal slices after incubation with p31-43 and p57-68 at different time points. Data obtained by western blotting analysis revealed that p31-43, but not p57-68, significantly increased Akt and Erk1/2 phosphorylation, whereas, conversely, we observed decreased p38 phosphorylation levels.

Moreover, the phosphorylation of the p65 subunit of the inflammatory marker NF $\kappa$ B resulted increased after p31-43, but not after p57-68 incubation. Similar results were obtained in *in vitro* studies using Caco-2 cell lines, usually used as model of intestinal epithelial cultures. Indeed, Capozzi and colleagues have shown that incubation with p31-43 (50  $\mu$ g/mL) for 45 min increases the expression of p65 NF $\kappa$ B [35]. In the same paper, the authors have also observed increased levels of ERK phosphorylation after p31-43 incubation, indicating that the MAPK pathway was also rapidly activated by p31-43 *in vitro* [35]. Importantly, the NF $\kappa$ B pathway is activated in the intestinal mucosa of untreated CD patients, and remains active even during the remission phase. This observation suggests that following the induction of the inflammatory response by gluten peptides, other mechanisms maintain an ongoing inflammatory process in the intestinal mucosa of CD patients regardless of the further gluten intake [36]. Furthermore, NF $\kappa$ B and MAPK pathways were also found active in fibroblasts derived from the skin and small intestine of CD patients [36]. Interestingly, none of the effects on NF $\kappa$ B or MAPK signalling were induced by the immunogenic peptide p57-68. Remarkably, p31-43 could activate the MAPK and NF $\kappa$ B pathways in cells from control subjects, suggesting that p31-43 "per se" has the ability to induce inflammation. In addition, studies using synthetic peptides containing alanine replacements along the p31-43 sequence demonstrated that the reported effects are specific for this peptide [37]. It was demonstrated that the canonical NF $\kappa$ B pathway regulates the expression of Transglutaminase 2 (TG2) gene; consequently, it can be induced by proinflammatory cytokines such as TNF $\alpha$  [38,39]. On the other hands, TG2 can activate NF $\kappa$ B by blocking the

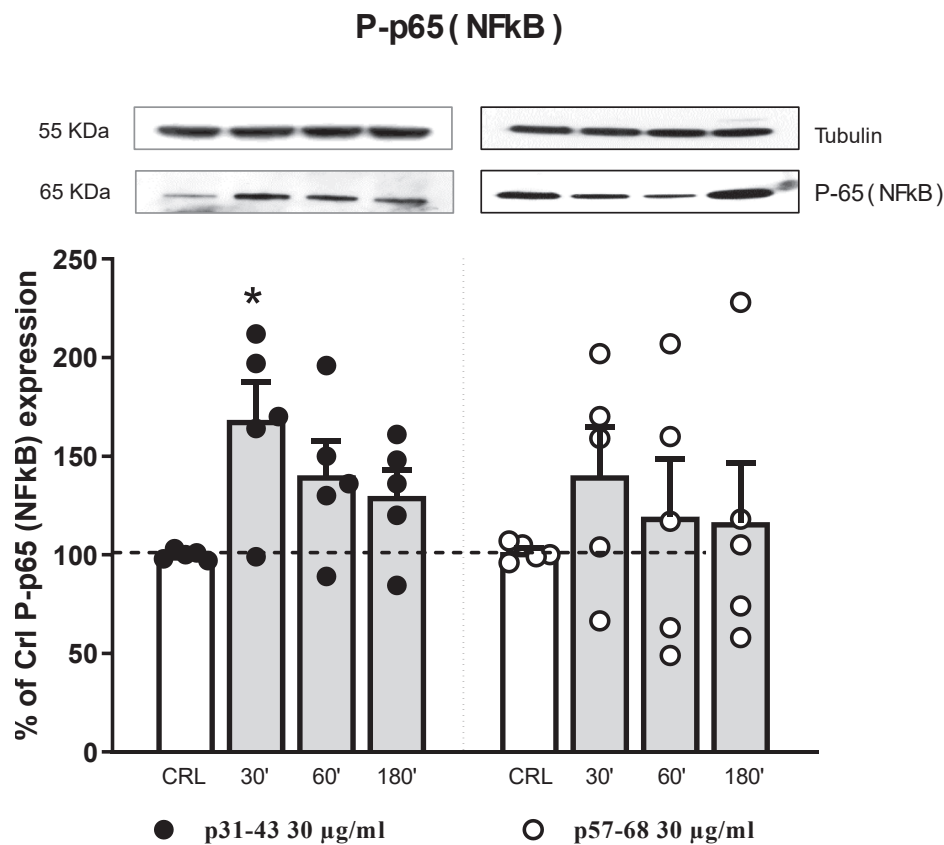


**Fig. 5.** Phosphorylation of the NFκB-subunit p65 is increased by p31-43 but not p57-68. Slices were exposed to p31-43 (grey column black circles) or to p57-68 (grey column white circles) for 30, 60 or 180 min and then processed for Western blotting. Representative immunoblots showing that p31-43 (left graph panel) but not p57-68 (right graph panel) increases the phosphorylation levels of the NFκB subunit p65. Data are expressed as percentage of control protein levels (white column). Bar represent the mean  $\pm$  SEM of three-five experiments from independent cell preparations (about  $\geq 8$  slices for each experimental point). \* $p < 0.05$  versus. CRL (ANOVA + Tukey's w test).

inhibitory function of IκBα leading to a complex cross-regulation between TG2 activity and the NFκB pathway [40]. All together, these evidence may explain the increased expression of TG2 induced by 24 h incubation with p31-43 in hippocampal slices [24] and could design an inflammatory signalling specifically activated by p31-43. These results suggest that the gliadin peptides p31-43 and p57-68 activates crucial but different pathways, that may be responsible for increased sensitivity to noxious stimuli.

Lastly, upon examining the impact of incubating p31-43 and p57-68 on the acetylation of nuclear histone-3 (k18), we observed a significant reduction solely induced by p31-43. Conversely, no changes were observed in the case of p57-68, indicating that the gliadin peptide p31-43 has the potential to induce epigenetic modifications. These findings suggest that p31-43 could serve as an epigenetic factor, capable of eliciting changes in gene expression that contribute to the pathophysiology of GRD. Epigenetic alterations, including histone acetylation, may offer insights into how genetic interactions with environmental factors contribute to the development of such diseases. Finally, given that oxidative stress has been proposed as a biomarker for monitoring treated celiac disease due to elevated levels of reactive oxygen species (ROS) and compromised antioxidant defense systems leading to tissue damage [41], we investigated the impact of p31-43 on oxidative status. Our findings revealed a significant increase in lipid peroxidation accompanied by a simultaneous decrease in total antioxidant capacity following p31-43 peptide incubation; thus corroborating previous observations by Luciani and colleagues, who reported that p31-43 accumulation in lysosomes activates intestinal epithelial cells via the ROS-TG2 axis [42].

Overall, these results highlight the differential sensitivity and tissue responses elicited by gliadin peptides, particularly emphasizing the

ability of p31-43 to independently activate central cellular signaling at both cytosolic and nuclear levels. Additional studies are needed to clarify the role of the gliadin peptides in the central nervous system and most importantly, their association with several neurological pathologies to which they may be associated. Undoubtedly, our study has a limitation in that the gliadin peptides were tested directly on brain tissue *in vitro*, assuming their ability to cross both the intestinal and blood-brain barrier. In this regards, however, there is evidence that p31-43 is able to cross the intestinal epithelium in duodenal biopsy specimens from patients of active celiac disease, and gliadin peptides have been detected in the pancreas of NOD and healthy mice following oral administration [43,44]. Moreover, it is important to acknowledge that the intestinal barrier is inherently flexible and responsive, as tight junctions can undergo changes in permeability due to various factors. These factors include pharmacological interventions (e.g., antibiotic therapy), dysbiosis, certain food items, or additive components (e.g., emulsifiers), as well as pathological conditions like acute and chronic inflammation, and stress. Therefore, the dynamic nature of the intestinal barrier should be taken into consideration. On the other hand, the blood-brain barrier is permeabilized by pathological situations, such as convulsions, but also altered by other factors. It is true that all scientific evidence is concerned with the concurrence of events, i.e. neuronal pathologies and GRD or CD. While gluten fragments themselves may not exhibit inherent toxicity, they have the potential to modify cell signaling and impact cellular responsiveness following an insult. In light of these findings, this study introduces several hypotheses and offers valuable insights into the mechanisms underlying the alterations and connections between gluten and neurological disorders. The results presented here provide a foundation for further investigation and contribute to our



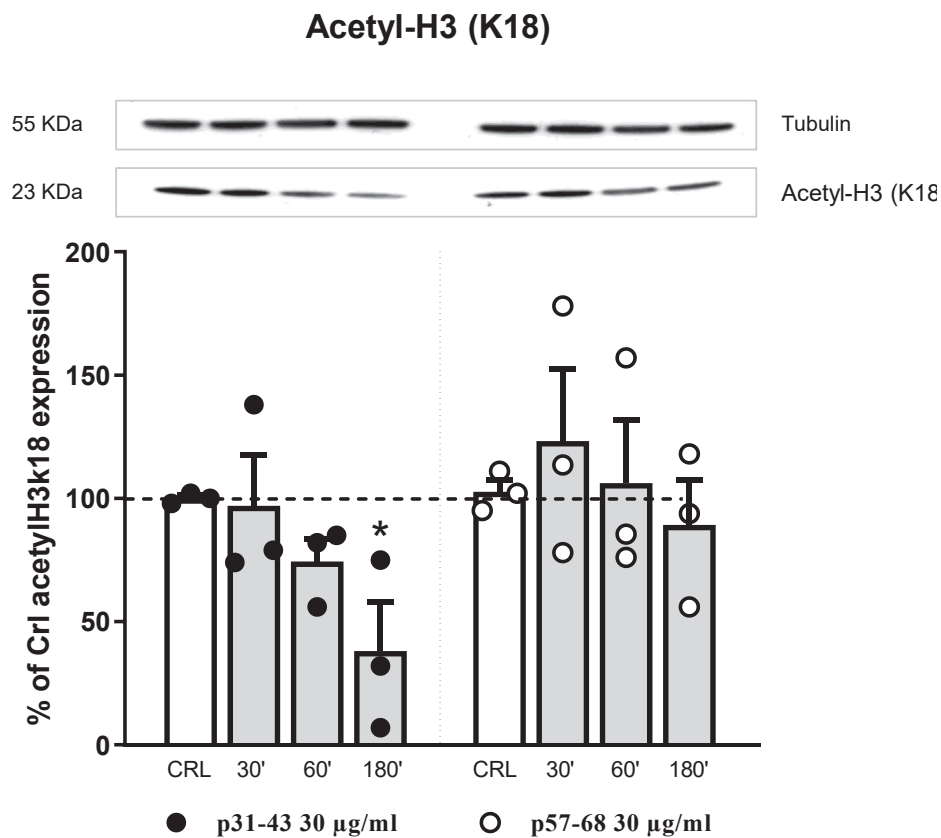


**Fig. 6.** Histone 3 acetylation is decreased by p31-43 but not p57-68. Slices were exposed to p31-43 (grey column black circles) or to p57-68 (grey column white circles) for 30, 60 or 180 min and then processed for Western blotting. Representative immunoblots showing that p31-43 (left graph panel) but not p57-68 (right graph panel) significantly reduces the acetylation levels of histone 3. Data are expressed as percentage of control protein levels (white column). Bar represent the mean ± SEM of three-five experiments from independent cell preparations (about ≥ 8 slices for each experimental point). \*p < 0.05 versus. CRL (ANOVA + Tukey's w test).

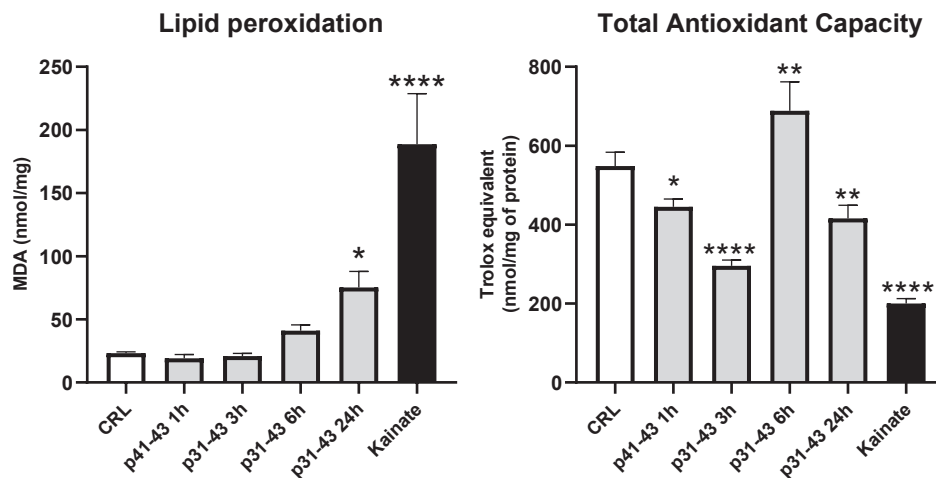


**Fig. 7.** P31-43 induces oxidative stress in organotypic hippocampal slices. Slices were exposed to p31-43 (grey column) for 1, 3, 6 or 24 h and then processed for lipid peroxidation and total antioxidant capacity assay. Bar graph show that p31-43 induces a significant increase in lipid peroxidation (left panel) complemented by a decrease in total antioxidant capacity (right panel). Bar represent the mean ± SEM of three experiments from independent cell preparations (about ≥ 4 slices for each experimental point). \*\*\*\*p < 0.001 and \*\*p < 0.01 and \*p < 0.05 versus. CRL (ANOVA + Dunnett's w test).

fundamental understanding of the complex interplay between gluten and the development of neurological conditions.

### 6. Funding and disclosures

This research was supported by grants from Fondazione Ente Cassa

di Risparmio di Firenze and Università degli Studi di Firenze (G.M.).

### Author contribution

EG designed the study, performed experiments and data analysis and wrote the first draft of the manuscript. MB performed experiments and

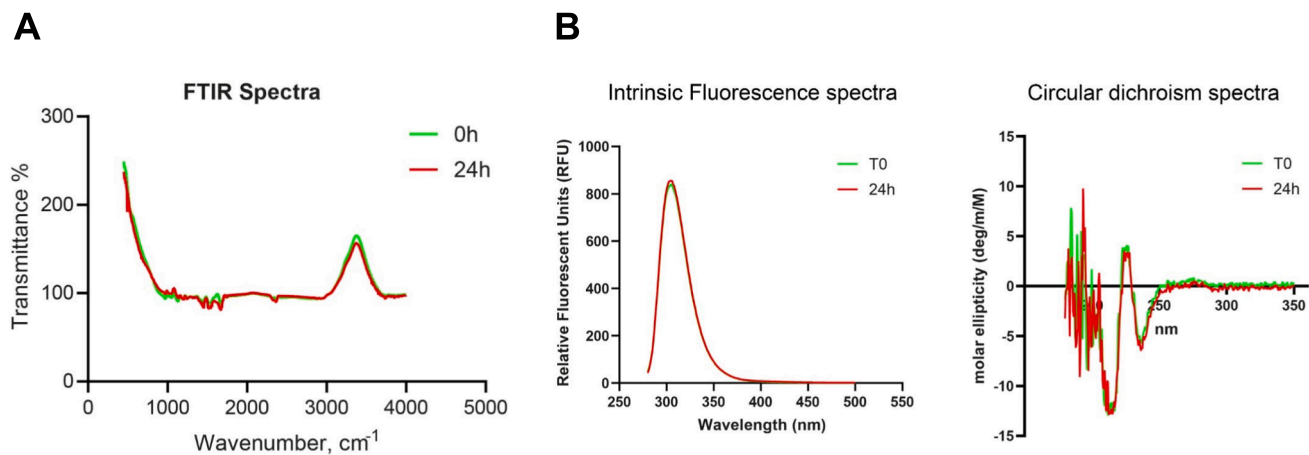


**Fig. 8.** Structural analysis of p31-43 aggregation. (A) Fourier Transform Infrared (FTIR) spectroscopy technique showing that p31-43 does not form aggregates under our experimental conditions. (B) Secondary structure of p31-43 analyzed by circular dichroism (CD) and intrinsic fluorescence (IF) spectroscopy at T0 and after 24 h of incubation at 37 °C in PBS showing that the recorded spectra are matching, demonstrating the absence of an aggregation process.

data analysis, contributed intellectually to the interpretation of the data and revised the manuscript. FR, DR, AC and GM contributed intellectually to the interpretation of the data and revised the manuscript. LC and GR performed experiments and AD performed peptide 3d images and contributed intellectually to the interpretation of the data. All authors have contributed to and approved the final manuscript.

#### CRedit authorship contribution statement

**Elisabetta Gerace:** Writing – review & editing, Writing – original draft, Supervision, Methodology, Investigation, Formal analysis, Data curation, Conceptualization. **Francesco Resta:** Writing – review & editing, Conceptualization. **Lorenzo Curti:** Writing – review & editing, Methodology, Formal analysis. **Alessandro Di Domizio:** Writing – review & editing, Data curation, Conceptualization. **Giuseppe Ranieri:** Methodology. **Matteo Becatti:** Writing – review & editing, Writing – original draft, Methodology, Formal analysis, Data curation. **Daniela Renzi:** Writing – review & editing, Conceptualization. **Antonino Calabrò:** Writing – review & editing, Visualization, Conceptualization. **Guido Mannaioni:** Writing – review & editing, Visualization, Resources, Funding acquisition, Conceptualization.

#### Declaration of competing interest

The authors declare that they have no known competing financial interests or personal relationships that could have appeared to influence the work reported in this paper.

#### Data availability

Data will be made available on request.

#### References

- [1] T. Hu, J. Zhang, J. Wang, L. Sha, Y. Xia, T.C. Ortyl, X. Tian, L. Chen, *Advances in Epilepsy: Mechanisms, Clinical Trials, and Drug Therapies*, *J. Med. Chem.* 66 (7) (2023) 4434–4467.
- [2] J.R. Jackson, W.W. Eaton, N.G. Cascella, A. Fasano, D.L. Kelly, *Neurologic and psychiatric manifestations of celiac disease and gluten sensitivity*, *Psychiatr. Q.* 83 (1) (2012) 91–102.
- [3] M. Hadjivassiliou, D.G. Rao, R.A. Grinewald, D.P. Aeschlimann, P.G. Sarrigiannis, N. Hoggard, P. Aeschlimann, P.D. Mooney, D.S. Sanders, *Neurological Dysfunction in Coeliac Disease and Non-Coeliac Gluten Sensitivity*, *Am. J. Gastroenterol.* 111 (4) (2016) 561–567.
- [4] M.D. Rouvroye, P. Zis, A.M. Van Dam, A.J.M. Rozemuller, G. Bouma, M. Hadjivassiliou, *The Neuropathology of Gluten-Related Neurological Disorders: A Systematic Review*, *Nutrients* 12 (3) (2020).
- [5] C. Briani, G. Zara, A. Alaedini, F. Grassivaro, S. Ruggero, E. Toffanin, M. P. Albergoni, M. Luca, B. Giometto, M. Ermani, F. De Lazzari, A. D'Orlando, L. Battistin, *Neurological complications of celiac disease and autoimmune mechanisms: a prospective study*, *J. Neuroimmunol.* 195 (1–2) (2008) 171–175.
- [6] G. Gobbi, F. Bouquet, L. Greco, A. Lambertini, C.A. Tassinari, A. Ventura, M. G. Zaniboni, *Celiac disease, epilepsy, and cerebral calcifications. The Italian Working Group on Coeliac Disease and Epilepsy*, *Lancet* 340 (8817) (1992) 439–443.
- [7] M. Peltola, K. Kaukinen, P. Dastidar, K. Haimila, J. Partanen, A.M. Haapala, M. Mäki, T. Keränen, J. Peltola, *Hippocampal sclerosis in refractory temporal lobe epilepsy is associated with gluten sensitivity*, *J. Neurol. Neurosurg. Psychiatry* 80 (6) (2009) 626–630.
- [8] H. Bashiri, D. Afshari, N. Babaei, M.R. Ghadami, *Celiac Disease and Epilepsy: The Effect of Gluten-Free Diet on Seizure Control*, *Adv. Clin. Exp. Med.* 25 (4) (2016) 751–754.
- [9] T. Julian, M. Hadjivassiliou, P. Zis, *Gluten sensitivity and epilepsy: a systematic review*, *J. Neurol.* 266 (7) (2019) 1557–1565.
- [10] D.S. Pengiran Tengah, A.J. Wills, G.K. Holmes, *Neurological complications of coeliac disease*, *Postgrad. Med. J.* 78 (921) (2002) 393–398.
- [11] A. Mavroudi, I. Xinias, T. Papastavrou, E. Karatza, M. Fotoulaki, C. Panteliadis, K. Spiroglou, *Increased prevalence of silent celiac disease among Greek epileptic children*, *Pediatr. Neurol.* 36 (3) (2007) 165–169.
- [12] J.V. Nadler, B.W. Perry, C.W. Cotman, *Intraventricular kainic acid preferentially destroys hippocampal pyramidal cells*, *Nature* 271 (5646) (1978) 676–677.
- [13] Y. Ben-Ari, *Limbic seizure and brain damage produced by kainic acid: mechanisms and relevance to human temporal lobe epilepsy*, *Neuroscience* 14 (2) (1985) 375–403.
- [14] Y. Ben-Ari, R. Cossart, *Kainate, a double agent that generates seizures: two decades of progress*, *Trends Neurosci.* 23 (11) (2000) 580–587.
- [15] V. Crépel, C. Mulle, *Physiopathology of kainate receptors in epilepsy*, *Curr. Opin. Pharmacol.* 20 (2015) 83–88.
- [16] R. Falcón-Moya, T.S. Sihra, A. Rodríguez-Moreno, *Kainate Receptors: Role in Epilepsy*, *Front. Mol. Neurosci.* 11 (2018) 217.
- [17] L. Shan, Ø. Molberg, I. Parrot, F. Hausch, F. Filiz, G.M. Gray, L.M. Sollid, C. Khosla, *Structural basis for gluten intolerance in celiac sprue*, *Science* 297 (5590) (2002) 2275–2279.
- [18] M.V. Barone, R. Troncone, S. Auricchio, *Gliadin peptides as triggers of the proliferative and stress/innate immune response of the celiac small intestinal mucosa*, *Int. J. Mol. Sci.* 15 (11) (2014) 20518–20537.
- [19] L. Maiuri, R. Troncone, M. Mayer, S. Coletta, A. Picarelli, M. De Vincenzi, V. Pavone, S. Auricchio, *In vitro activities of A-gliadin-related synthetic peptides: damaging effect on the atrophic coeliac mucosa and activation of mucosal immune response in the treated coeliac mucosa*, *Scand. J. Gastroenterol.* 31 (3) (1996) 247–253.
- [20] P.J. Ciclitira, H.J. Ellis, *In vivo gluten ingestion in coeliac disease*, *Dig. Dis.* 16 (6) (1998) 337–340.
- [21] L. Maiuri, C. Ciacci, I. Ricciardelli, L. Vacca, V. Raia, S. Auricchio, J. Picard, M. Osman, S. Quarantino, M. Londei, *Association between innate response to gliadin and activation of pathogenic T cells in coeliac disease*, *Lancet* 362 (9377) (2003) 30–37.
- [22] F.G. Chirido, S. Auricchio, R. Troncone, M.V. Barone, *The gliadin p31–43 peptide: Inducer of multiple proinflammatory effects*, *Int. Rev. Cell Mol. Biol.* 358 (2021) 165–205.
- [23] J.A. Tye-Din, J.A. Stewart, J.A. Dromey, T. Beissbarth, D.A. van Heel, A. Tatham, K. Henderson, S.I. Mannering, C. Gianfrani, D.P. Jewell, A.V. Hill, J. McCluskey, J. Rossjohn, R.P. Anderson, *Comprehensive, quantitative mapping of T cell epitopes in gluten in celiac disease*, *Sci. Transl. Med.* 2 (41) (2010) 41ra51.

- [24] E. Gerace, F. Resta, E. Landucci, D. Renzi, A. Masi, D.E. Pellegrini-Giampietro, A. Calabrò, G. Mannaioni, The gliadin peptide 31–43 exacerbates kainate neurotoxicity in epilepsy models, *Sci. Rep.* 7 (1) (2017) 15146.
- [25] E. Gerace, E. Landucci, T. Scartabelli, F. Moroni, D.E. Pellegrini-Giampietro, Rat hippocampal slice culture models for the evaluation of neuroprotective agents, *Methods Mol. Biol.* 846 (2012) 343–354.
- [26] M. Morin-Brureau, F. De Bock, M. Lerner-Natoli, Organotypic brain slices: a model to study the neurovascular unit micro-environment in epilepsies, *Fluids Barriers CNS* 10 (1) (2013) 11.
- [27] D.E. Pellegrini-Giampietro, F. Peruginelli, E. Meli, A. Cozzi, S. Albani-Torregrossa, R. Pellicciari, F. Moroni, Protection with metabotropic glutamate 1 receptor antagonists in models of ischemic neuronal death: time-course and mechanisms, *Neuropharmacology* 38 (10) (1999) 1607–1619.
- [28] D. Cavallo, E. Landucci, E. Gerace, D. Lana, F. Ugolini, M.F. Henley, M. G. Giovannini, D.E. Pellegrini-Giampietro, Neuroprotective effects of mGluR5 activation through the PI3K/Akt pathway and the molecular switch of AMPA receptors, *Neuropharmacology* 162 (2020) 107810.
- [29] E. Gerace, E. Landucci, T. Scartabelli, F. Moroni, A. Chiarugi, D.E. Pellegrini-Giampietro, Interplay between histone acetylation/deacetylation and poly(ADP-ribosylation) in the development of ischemic tolerance in vitro, *Neuropharmacology* 92 (2015) 125–134.
- [30] D. Ami, A. Natalello, Characterization of the Conformational Properties of Soluble and Insoluble Proteins by Fourier Transform Infrared Spectroscopy, *Methods Mol. Biol.* 2406 (2022) 439–454.
- [31] P. Zis, M. Hadjivassiliou, Treatment of Neurological Manifestations of Gluten Sensitivity and Coeliac Disease, *Curr. Treat. Options. Neurol.* 21 (3) (2019) 10.
- [32] A.C. Whitebitch, B. Santoro, A. Barnett, C.P. Lisgaras, H.E. Scharfman, S. A. Siegelbaum, Reduced Cholecystokinin-Expressing Interneuron Input Contributes to Disinhibition of the Hippocampal CA2 Region in a Mouse Model of Temporal Lobe Epilepsy, *J. Neurosci.* 43 (41) (2023) 6930–6949.
- [33] A. Kiliyas, S. Tulke, N. Barheier, P. Ruther, U. Häussler, Integration of the CA2 region in the hippocampal network during epileptogenesis, *Hippocampus* 33 (3) (2023) 223–240.
- [34] L. Calvanese, M. Nanayakkara, R. Aitoro, M. Sanseverino, A.L. Tornesello, L. Falcigno, G. D'Auria, M.V. Barone, Structural insights on P31–43, a gliadin peptide able to promote an innate but not an adaptive response in celiac disease, *J Pep Sci.* 25 (2019) e3161.
- [35] A. Capozzi, O. Vincentini, P. Gizzi, A. Porzia, A. Longo, C. Felli, V. Mattei, F. Mainiero, M. Silano, M. Sorice, R. Misasi, Modulatory Effect of Gliadin Peptide 10-mer on Epithelial Intestinal CACO-2 Cell Inflammatory Response, *PLoS One* 8 (6) (2013) e66561.
- [36] A. Castellanos-Rubio, J.R. Bilbao, Profiling Celiac Disease-Related Transcriptional Changes, *Int. Rev. Cell Mol. Biol.* 336 (2018) 149–174.
- [37] G. Lania, M. Nanayakkara, M. Maglio, R. Auricchio, M. Porpora, M. Conte, M.A. De Matteis, R. Rizzo, A. Luini, V. Discepolo, R. Troncone, S. Auricchio, M.V. Barone, Constitutive alterations in vesicular trafficking increase the sensitivity of cells from celiac disease patients to gliadin, *Commun Biol* 2 (2019) 190.
- [38] M. Bayardo, F. Punzi, C. Bondar, N. Chopita, F. Chirido, Transglutaminase 2 expression is enhanced synergistically by interferon- $\gamma$  and tumour necrosis factor- $\alpha$  in human small intestine, *Clin. Exp. Immunol.* 168 (1) (2012) 95–104.
- [39] J. Lee, Y.S. Kim, D.H. Choi, M.S. Bang, T.R. Han, T.H. Joh, S.Y. Kim, Transglutaminase 2 induces nuclear factor-kappaB activation via a novel pathway in BV-2 microglia, *J. Biol. Chem.* 17;279(51) (2004) 53725–53735.
- [40] S. Moretti, S. Mrakic-Spota, L. Roncoroni, A. Vezzoli, C. Dellanoce, E. Monguzzi, F. Branchi, F. Ferretti, V. Lombardo, L. Doneda, A. Scricciolo, L. Elli, Oxidative stress as a biomarker for monitoring treated celiac disease, *Clin. Transl. Gastroenterol.* 9 (6) (2018) 157.
- [41] A. Luciani, V.R. Villella, A. Vasaturo, I. Giardino, M. Pettoello-Mantovani, S. Guido, O.N. Cexus, N. Peake, M. Londei, S. Quarantino, L. Maiuri, Lysosomal accumulation of gliadin p31–43 peptide induces oxidative stress and tissue transglutaminase-mediated PPARgamma downregulation in intestinal epithelial cells and coeliac mucosa, *Gut* 59 (3) (2010) 311–319.
- [42] C. Lebreton, S. Menard, J. Abed, I. Cruz Mora, R. Coppo, C. Dugave, R.C. Monteiro, A. Fricot, M. Garfa Traore, M. Griffin, C. Cellier, G. Malamut, N. Cerf-Bensussan, M. Heiman, Interactions Among Secretory Immunoglobulin A, CD71, and Transglutaminase-2 Affect Permeability of Intestinal Epithelial Cells to Gliadin Peptides, *Gastroenterology* 143 (2012) 698–707.
- [43] S.W. Bruun, K. Josefsen, J.T. Tanassi, A. Marek, M.H.F. Pedersen, U. Sidenius, M. Haupt-Jorgensen, J.C. Antvorskov, L. Larsen, N.H. Heegaard, K. Buschard, Large Gliadin Peptides Detected in the Pancreas of NOD and Healthy Mice following Oral Administration, *J Diabete Res.* 2016 (2016) 2424306.
- [44] W. Humphrey, A. Dalke, K. Schulten, VMD: visual molecular dynamics, *J Mol Graph.* 14(1) (1196) 33-8, 27-8.